1-1-2010

Diffusion of the Cu monomer and dimer on Ag(111): Molecular dynamics simulations and density functional theory calculations

Sardar Sikandar Hayat

Marisol Alcántara Ortigoza
University of Central Florida

Muhammad A. Choudhry

Talat S. Rahman
University of Central Florida

Diffusion of the Cu monomer and dimer on Ag(111): Molecular dynamics simulations and density functional theory calculations

Sardar Sikandar Hayat*
Department of Physics, The Islamia University of Bahawalpur, Bahawalpur 63120, Punjab, Pakistan

Marisol Alcántara Ortigoza†
Department of Physics, University of Central Florida, Orlando, Florida 32816, USA

Muhammad A. Choudhry‡
Department of Physics, The Islamia University of Bahawalpur, Bahawalpur 63120, Punjab, Pakistan

Talat S. Rahman§
Department of Physics, University of Central Florida, Orlando, Florida 32816, USA
(Received 19 December 2008; revised manuscript received 19 June 2010; published 3 August 2010)

We present results of molecular dynamics (MD) simulations and density functional theory (DFT) calculations of the diffusion of Cu adatom and dimer on Ag(111). We have used potentials generated by the embedded-atom method for the MD simulations and pseudopotentials derived from the projected-augmented-wave method for the DFT calculations. The MD simulations (at three different temperatures: 300, 500, and 700 K) show that the diffusivity has an Arrhenius behavior. The effective energy barriers obtained from the Arrhenius plots are in excellent agreement with those extracted from scanning tunneling microscopy experiments. While the diffusion barrier for Cu monomers on Ag(111) is higher than that reported (both in experiment and theory) for Cu(111), the reverse holds for dimers [which, for Cu(111), has so far only been theoretically assessed]. In comparing our MD result with those for Cu islets on Cu(111), we conclude that the higher barriers for Cu monomers on Ag(111) results from the comparatively large Ag-Ag bond length, whereas for Cu dimers on Ag(111) the diffusivity is taken over and boosted by the competition in optimization of the Cu-Cu dimer bond and the five nearest-neighbor Cu-Ag bonds. Our DFT calculations confirm the relatively large barriers for the Cu monomer on Ag(111)—69 and 75 meV—compared to those on Cu(111) and hint a rationale for them. In the case of the Cu dimer, the relatively long Ag-Ag bond length makes available a diffusion route whose highest relevant energy barrier is only 72 meV and which is not favorable on Cu(111). This process, together with another involving an energy barrier of 83 meV, establishes the possibility of low-barrier intercell diffusion by purely zigzag mechanisms.

DOI: 10.1103/PhysRevB.82.085405 PACS number(s): 68.35.Fx, 36.40.Sx, 68.55.A−

I. INTRODUCTION

The diffusivity of monomers and small adatom clusters is the key controlling factor in island nucleation and hence growth. The importance of these dynamical processes extends, for example, to metal oxidation rates[1,2] and functionality (catalytic, magnetic, etc.) of supported heterogeneous materials when surface/volume ratio and/or a complex structural pattern formation become important.[3,4] A good deal of work has thus been dedicated to explaining the motion of adatom clusters on surfaces in homoepitaxial metallic systems[5–21] and, more recently, in heteroepitaxial systems.[15,22–25] Heteroepitaxy of course exhibits a broad variety of growth modes and diffusion processes but, at the same time, introduces factors beyond those that need be considered in homoepitaxial models in order to comprehend the diffusivity of adatom clusters. Growth of Cu on Ag is a particularly striking example of heteroepitaxy subject to effects caused by bond-length misfit (13.5%) and by binding-energy disparity [cohesive energy difference of 0.83 eV and surface energy difference of 0.15 eV (Ref. 26)] between the two metals involved.

One way to approach the problem of identifying the processes that govern diffusivity and of calculating their energy barriers is by using the classical molecular dynamics (MD) method. Such an approach is appropriate for achieving understanding of thermally driven kinetic phenomena whose description is beyond the reach of *ab initio* methods and/or currently available computational capabilities.[10,12,20] This is particularly true for heterogeneous systems in which the lattice mismatch may be problematic for methods such as kinetic Monte Carlo.[27] Some progress has already been achieved recently in describing diffusion and growth in heterogeneous systems: Goyhenex[24] relates the greater mobility of Co dimers with respect to that of Pt dimers on Pt(111) to the lattice mismatch; Bocquet *et al.*[23] have successfully used MD simulations to confirm the experimental observation that proximity of Cu adatom islands to surface steps on Ag(111) induces the Ag step atoms to spill over the Cu islands.

Nevertheless, the major disadvantages to using MD simulation for modeling the systems of interest here derive from the fact that measurements of surface diffusion using scanning-tunneling microscopy (STM) are performed at low temperatures (5–25 K) and typically over times from milliseconds to hours. Classical MD cannot capture any quantum phenomena that may emerge at such low temperatures, and is limited by computing resources to simulations over time and length scales that differ from those in experiments by several orders of magnitude. One way to address the short duration of the MD simulations (on the order of nanosecond) has been to perform them at much higher temperatures (above room temperature) so as to accelerate atomic processes which have relatively high activation energy barriers. Recent advances in computational hardware and software have certainly helped somewhat overcome the restriction traditionally attached to MD simulations by making simulations of systems containing a few thousand atoms feasible for longer time scales ($\sim$10–100 ns) on small computer clusters in reasonable real time. An important and promising result concerning the differences in temperature ranges between MD simulations and experiments was that first provided by Kürpick and Rahman,[28] who found that MD and molecular-statics calculations produce the same energy barriers for monomer self-diffusion on Ag(001). The same occurs for self-diffusion on the (001), (110), and (111) surfaces of Cu, Ag, and Ni (see Ref. 29, and references therein). However, Kürpick *et al.*[30] found—via the transition state theory and the local thermodynamic functions of the system—that, while the prefactors are temperature independent above room temperature and tend to the Vineyard's expression,[31] they steeply increase for hopping and decrease for exchange, as temperature decreases. Another limitation to the predictive power of MD simulations is the reliance of the results upon the choice of interatomic potentials. Nonetheless, semiempirical many-body interaction potentials, such as those obtained by the embedded-atom method (EAM),[32] have overcome some of the basic objections against the use of conventional pair potentials. In fact, about two decades of work using MD simulations based on many-body interatomic potentials has established them as a dependable approach for evaluating microscopic properties of certain fcc metals. In fact, it has been shown[14,33,34] that there are only subtle differences in the activation energy barriers obtained from *ab initio* methods and those from many-body-interaction potentials. A larger discrepancy in the energy barriers may come from the choice of the approximation for the exchange-correlation functional [local-density approximation vs generalized gradient approximation (GGA)] in density functional theory (DFT).[28] Moreover, in this work we show that surface energetics obtained using *ab initio* methods validate those obtained from EAM potentials. In brief, even though MD still has serious limitations, the above-cited and many other similar studies using MD also demonstrate the power of this approach.

Morgenstern *et al.*[22,35] have recently assessed experimentally the diffusion barriers of Cu monomers and dimers on Ag(111) by means of low-temperature STM. The diffusivity of Cu monomers and dimers was monitored as a function of surface temperature only from 6 to 25 K, since clusters this small attach easily to Ag surface steps or larger Cu islands above 25 K and thus disappear from the Ag(111) terraces.[22] In the above range of temperature, Morgenstern *et al.*[35] determined that monomer diffusion occurs mostly via fcc$\leftrightarrow$fcc hopping with a barrier of 65 ± 9 meV. They identified the zigzag motion in turn as the leading diffusion process for dimers and estimated for it an energy barrier of $\sim$73 meV.[22,35] A puzzling finding in this work is that, from 21 to 24 K, long-range interactions among monomers (at distances $\geq$17 Å), between monomers and dimers, and among dimers (at distances $\geq$37 Å) markedly quench the hopping of monomers and the intracell and intercell processes of dimers.[22] Monomer-monomer interactions were accounted for by electric dipole-dipole, elastic, (arising from the substrate deformation) and/or Friedel-type interactions. However, the issue of why the monomer-dimer and dimer-dimer interactions are stronger and have even longer range than those between monomers remains unsettled.[22]

On the theoretical side, to our knowledge, only the molecular statics calculations (using potentials obtained via the effective-medium theory) performed by Morgenstern *et al.*[35] have addressed the Cu adatom and dimer diffusion on Ag(111). In agreement with experiment, the calculated diffusion barrier for Cu monomers on Ag(111) (80 meV) is higher than that on Cu(111) ($\sim$40–50 meV).[11,36–38] Concerning Cu dimers on Ag(111), the above calculations found the barrier for the zigzag motion to be 120 meV and that for concerted motion to be $\sim$140 meV.[35] While the slightly lower barrier for the zigzag motion made it the more favorable one, it is not completely clear what the leading dimer-diffusion mechanisms are, since the calculated diffusion barrier for the zigzag process is $\sim$1.7 times the experimental result, a discrepancy indicative of the presence of additional or different processes controlling the dimer diffusivity. Turning to our comparison with Cu/Cu(111), the fact that zigzag processes may play an important role in the diffusion of the Cu dimer on Ag(111) (Ref. 35) actually comes as a surprise since concerted motion has been considered to be the chief diffusion mechanism for Cu dimers on Cu(111).[11,37] Kinetic Monte Carlo calculations,[36] for example, found that the effective diffusion barrier for the Cu dimer on Cu(111) (92 meV), in which low-energy zigzag processes are allowed to intervene, is only 9 meV lower than that for the concerted motion alone, from fcc-fcc to hcp-hcp and from hcp-hcp to hcp-hcp. Recent MD simulations[38] of up to 1 μs have obtained a diffusion barrier for the Cu dimer on Cu(111) of $\sim$125 meV, thus confirming the effective diffusion barriers reported by Karim *et al.*,[36] Chang *et al.*,[11] and Marinica *et al.*[37] The above results thus indicate that the role of zigzag and other processes is minor in the diffusion of the Cu dimer on Cu(111).[36] Note that a previous simulation of up to 2.5 ns that considered the number of hopping events instead of the mean-square displacement of the center of mass in order to determine the diffusion coefficient, produced a much lower value: $\sim$74 meV.[39]

Our aim in this work is to attain understanding of the microscopic processes responsible for the diffusive behavior observed for Cu monomers and dimers on Ag(111) (Refs. 22 and 35) and, thereby, of the early stages of the heteroepitaxial growth. To this end, we have calculated the diffusion coefficient of the monomer and dimer for three temperatures—300, 500, and 700 K—based on MD simulations within the framework of EAM potentials. In order to shed light on our MD simulations, we have employed DFT to explore the potential-energy surface for a Cu monomer and a Cu dimer on Ag(111). To this end, we have searched for the transition states and energy barriers of relevant processes.

The rest of the paper is organized as follows: Sec. II provides the particulars of our MD and our first-principles calculations, respectively. Section III summarizes the results of our MD calculations of the diffusion coefficients, effective energy barriers, diffusion prefactors of the Cu monomer and dimer as a function of temperature, and discusses the processes identified for the monomer and dimer. Section IV presents the results of our first-principles calculations. Finally, Sec. V summarizes our findings and offers concluding remarks.

II. COMPUTATIONAL DETAILS

A. Molecular dynamics calculations

Since details of the MD technique can be found readily in textbooks, we confine ourselves to merely summarizing the salient features of the procedure applied in the present study. We simulate the diffusion of the Cu monomer and dimer on Ag(111) using a periodic supercell containing a six-layer Ag slab of 400 atoms (20×20) per layer. Thus the Cu monomer corresponds to a coverage of 2.5×10^{-3} ML. Cu adatoms are placed on only one side of the slab. Periodic boundary conditions are applied in the direction parallel to the surface but not in the direction perpendicular to the surface. The Cu monomer and dimer are placed randomly on the Ag(111) surface in their minimum-energy configurations at 0 K obtained via the conjugate-gradient algorithm.[40] Next, the system is thermalized during a 20 ps run keeping constant the number of atoms, the volume, and the temperature. Finally, we execute constant-energy MD runs—at 300, 500, and 700 K—to monitor the diffusion of the monomer and dimer for 6 ns. We apply the Nordsieck algorithm[41] to solve the classical equations of motion with a time step of 1 fs, recording statistics after every 0.05 ps at each temperature.

The diffusion coefficient, D, was calculated at each temperature according to the definition,

$$D=\lim_{t\to\infty}\frac{\langle[R_{CM}(t)-R_{CM}(0)]^2\rangle}{2dt}, \quad (1)$$

where $R_{CM}(t)$ is the position of the adatom or of the center of mass of the dimer at time t and d is the dimensionality of the system. The values of the effective diffusion energy barriers and the diffusion prefactors are derived from the Arrhenius plot of D as a function of temperature, namely, $\ln(D)=\ln(D_0)+\Delta E/k_BT$, where D_0 is the diffusion prefactor, ΔE is the effective energy barrier, k_B is the Boltzmann constant, and T is the temperature.

The atomic interaction is modeled through many-body potentials obtained via EAM.[32] The embedding functions, the atomic densities, and the pair-interaction functions for modeling Ag and Cu atoms are built in accordance with the parameters given in Ref. 42. The potentials of Ag and Cu so constructed are minimized at a lattice parameter of 4.09 Å and 3.62 Å, respectively, at 0 K. For finite-temperature calculations, we obtain the appropriate lattice parameter of the Ag substrate by simulating fcc bulk Ag with a periodic cubic supercell at constant number of atoms (256), pressure, and temperature. We find the lattice parameter of Ag to expand by 0.6%, 1.0%, and 1.5% at 300 K, 500 K, and 700 K, respectively, with respect to that at 0 K.

B. First-principles calculations of diffusion energetics

Our calculations have been carried out using DFT and the plane-wave pseudopotential method[43] as embodied in the code VASP (Ref. 44) with projected-augmented-wave-method pseudopotentials. We have used a supercell composed of a five-layer Ag(111) slab and a vacuum layer of 14 Å in order to maintain the periodicity of the system along the direction perpendicular to the surface. A Cu monomer and a dimer were adsorbed at various sites on the Ag(111) substrate. To diminish interaction between the Cu adatoms in the periodic images of the supercell, the (111) surface was extended to a (3×3) superstructure. With such a geometry, the shortest distance between Cu atoms of neighboring dimers is little more than two Ag-Ag bond lengths. The supercell thus contained 45 Ag atoms, plus either a Cu monomer or a dimer. The Brillouin zones were sampled with $(4\times4\times1)$ Monkhorst-Pack k-point meshes.[45] We used a kinetic-energy cutoff of 400 eV for the wave functions and 10 000 eV for the charge density in order to ensure sufficient computational accuracy. We used the Perdew-Burke-Ernzerhof GGA (Ref. 46) for the exchange-correlation functional.

We used the conjugated-gradient algorithm[40] to relax the structure of the systems studied in this work. At equilibrium, forces on each atom are required to be below 0.001 eV/Å. The diffusion barriers for monomers and dimers on the Ag(111) surface are determined by the dragging method: one obtains the total energy of the system at each point along the chosen diffusion path by fixing the coordinate of the Cu adatom along that path and allowing its other coordinates and those of all other atoms in the system to relax.

III. RESULTS AND DISCUSSION OF MD SIMULATIONS

In this section we first provide general remarks about our calculated diffusion coefficients and energy barriers. We then introduce the grounds on which our results will be interpreted. Next, we describe the effect of the diffusion of the Cu monomer and dimer on Ag(111) observed in our MD simulations and its possible link with the long range monomer-dimer and dimer-dimer interactions observed in experiment.[22] Subsequently, Secs. III A and III B focus on the observed diffusion mechanisms for the Cu monomer and dimer on Ag(111). There, we also analyze the origin of the differences between Cu(111) and Ag(111) with regard to the energy barriers that these two substrates set for the diffusion of the Cu monomer and dimer. In the rest of the paper, we will use an abbreviated notation to describe the adatoms sites—f for fcc, h for hcp, and b for bridge. For instance, the dimer site is said to occupy an "ff site" if both atoms sit at fcc sites.

The diffusion coefficients D for the Cu monomer and dimer on Ag(111) obtained from our MD simulations at the three temperatures are summarized in Table I. From several sets of simulations we find the error in D to be less than 3% for the monomer and 5% for the dimer. Extraction of the effective diffusion energy barrier ΔE and the diffusion prefactor D_0 for the Cu monomer and dimer (see Table I) is enabled by the smooth Arrhenius behavior[21] of the diffusion coefficient D (in Fig. 1). The negligible temperature depen-

TABLE I. Diffusion coefficient (D) at 300, 500, and 700 K; effective energy barrier (ΔE); and diffusion prefactor (D_0) of the Cu monomer and dimer on Ag(111).

	D (Å^2/s)				
	300 K	500 K	700 K	ΔE (meV)	D_0 (Å^2/s)
Cu_1	4.56×10^{11}	1.14×10^{12}	1.68×10^{12}	59	4.49×10^{12}
Cu_2	3.07×10^{11}	9.59×10^{11}	1.53×10^{12}	73	4.14×10^{12}

dence of the prefactors between ~300 and 600 K is well understood since this temperature range is low enough that the potential energy of the entire crystal can be considered harmonic[31,47] and the atomic vibrations treated as small oscillations[31] while high enough that quantum effects may be neglected.[31] The temperature independence of the prefactors, however, cannot be extrapolated to low temperatures, such as those at which the experiments of interest here are performed (25 K), since the vibrational states—many of which are unoccupied at 25 K—must be described quantum mechanically.[29] It is noteworthy that MD simulations by Ferrón *et al.*[48] have found that above 300 K long and recrossing jumps for the diffusion of a Cu adatom on Cu(111) lead to deviation of D from the Arrhenius behavior obtained from 100 to 250 K. The calculated effective energy barriers in turn may be extrapolated down to zero temperature because their temperature dependence arises only from the expansion of the lattice, which is smaller from 0 to 300 K than from 300 to 700 K (see Sec. II A).

A useful point of departure for understanding the kinetics of Cu monomers and dimers on Ag(111) (Secs. III A and III B) is the contrast with the corresponding homoepitaxial case Cu/Cu(111), for which a considerable body of theoretical and experimental work is already available.[11,12,36,37,49–52] The interpretation of our results outlined below is reached as well in the light of a recent study[53] on a $Ag_{27}Cu_7$ core-shell nanoparticle, which suggests that there is a bond-strength hierarchy among homobonds and heterobonds that mediates the minimum-energy structure of any particular system. Such a hierarchy in Ag-Cu systems largely favors the optimization of Cu-Cu bonds over that of Ag-Ag bonds, while the Cu-Ag bonds, if not constrained by the symmetry of the system, may be almost as short and strong as the Cu-Cu bonds. For this reason, the relatively weak and loose Ag-Ag bonds (as compared to Cu-Cu and Cu-Ag bonds) easily give way to reducing Cu-Cu and/or Cu-Ag bond lengths down to the bond length of bulk Cu, often at the expense of expanding the Ag-Ag bonds of those Ag atoms which make bonds with Cu atoms (see Ref. 54).

Concerning the effects of the diffusion of a Cu monomer and dimer on Ag(111), we observe that both perturb the structure of the Ag substrate as function of their instant position and configuration. These changes in the structure of the Ag substrate increase with temperature and are distinct for the monomer and dimer. The perturbation is particularly conspicuous for the dimer in which case the dislocations clearly do not remain local. Snapshots of our simulations show that some hollow sites on Ag(111), separated from the Cu dimer by about 3–43 Å and at apparently uncorrelated positions, are considerably enlarged during the vibration, rotation, and diffusion of the dimer (see Fig. 2). Such hollow sites may be localized or run as fissures along the $[\bar{1}01]$, $[0\bar{1}1]$, and $[\bar{1}10]$ directions, often parallel to the axis of the dimer bond. Notice that the terms "fissures" and "dislocations" in this context do not mean that the dimer causes a crystallographic defect on the surface as a result of the rupture of the Ag-Ag bonds along a line in the lattice. They mean only that the dimer gives rise to vibrations of the substrate whose displacement patterns expand and contract the Ag-Ag bonds along a line in the lattice. That fissures do not always run along the orientation of the dimer is probably because the response time of the surface is history dependent. A careful examination of our simulations suggests that the dislocations propagate out of the Cu adatoms as though a cylindrical elastic field[55] were radiated in response to the geometrical changes (vibration, rotation, and translation) experienced by the Cu dimer. Nevertheless, no definite far-field

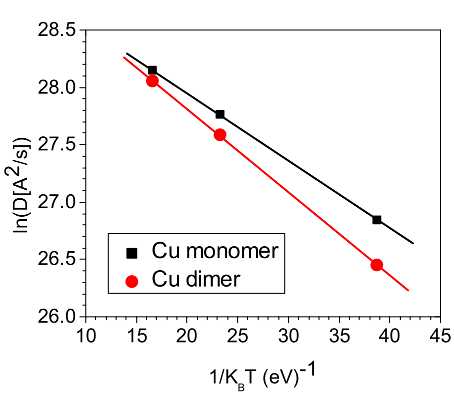

FIG. 1. (Color online) Arrhenius plot of the diffusion coefficient of Cu monomer and dimer on Ag(111).

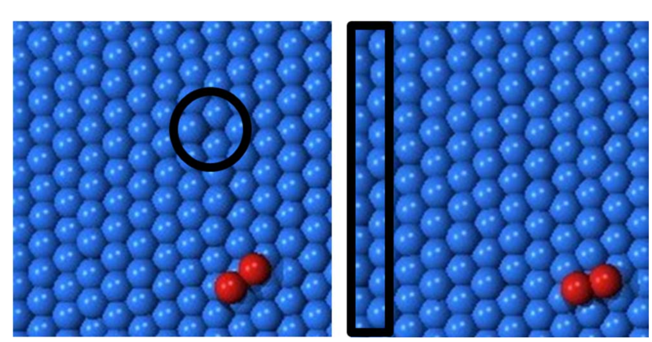

FIG. 2. (Color online) Dislocations and fissures of the Ag(111) substrate at distances from 3 to 43 Å from the Cu dimer during its vibration, rotation, and diffusion at 300 K (see text).

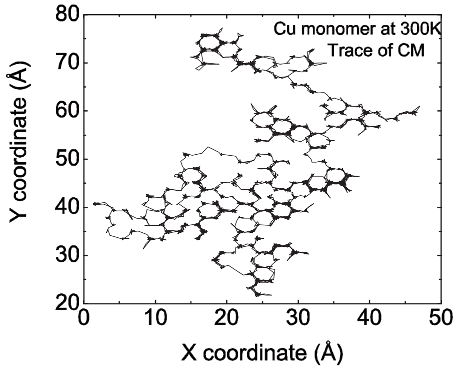

FIG. 3. Trace of the center of mass of the Cu monomer on Ag (111) at 300 K for 2000 ps.

pattern was recognized. One reason may be that the *source* of the elastic field—the motion of the adatoms—is random and far more complicated than point sources (monopole, dipole, etc.). Also, considering the long range of the perturbations, one may expect that the periodic boundary conditions yield to interference before the displacement waves die off.

The above features may be unanticipated since the range of the potentials used in this work does not go beyond 5.5 Å (i.e., the fourth-neighbor shell).[42] Moreover, Feibelman has demonstrated that long-range force constants beyond the fourth-nearest-neighbor (NN) shell are governed by Friedel oscillations,[56] which are not taken into account in the EAM potentials used in this work. Nevertheless, point defects such as impurities may scatter bulk and surface modes, thus introducing new vibrational modes in their vicinity,[57,58] which may, incidentally, be occupied at low temperatures (16–25 K).[57] Adatom impurities are hence localized perturbations of the periodic potential that oscillate randomly and may generate an elastic displacement field that is dynamically active, falls off at large distances (larger than those expected in Ref. 22), and may therefore be involved in the long-range monomer-dimer and dimer-dimer interactions detected in experiment.[22]

A. Monomer

With respect to the diffusion mechanisms for a Cu monomer on Ag(111), we observe that the monomer visits both f and h sites. The trace of the center of mass of the Cu monomer thus forms hexagons as it diffuses on Ag (111) (see Fig. 3). Our MD simulation at 300 K, however, shows that the Cu monomer hops to and stays on f sites approximately two times more than on h sites.[54] In experiment, in contrast, monomers visit f sites more often than h sites by a factor of 35 at 21 K.[22] In the homoepitaxial case, even though the $f \leftrightarrow f$ hopping on Cu(111) is triggered at $\sim$11 K—i.e., at a temperature 4 K lower than found for Ag(111),[22] the $h \rightarrow f$ hopping rate of a Cu monomer on Cu(111) (obtainable only through Cu adatom lateral manipulation) is at least 75 times larger than that of $f \rightarrow h$ hopping.[49] We conclude that since the instability of the h site in the homoepitaxial case derives from the repulsive interaction with the atom directly below, the short length of optimized Cu-Ag bonds,[53] compared to the length of Ag-Ag bonds, helps stabilize the h site in the heteroepitaxial case.

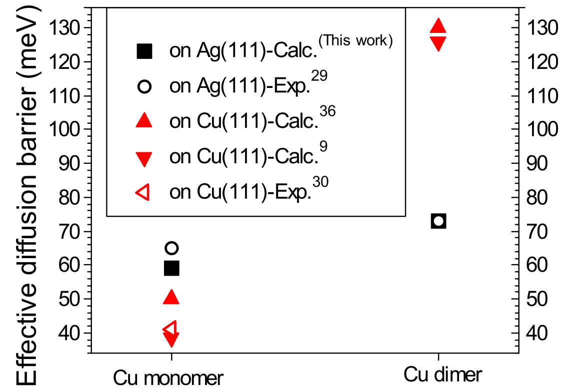

FIG. 4. (Color online) The effective diffusion barriers of Cu monomers and dimers on Ag(111) are compared to those on Cu(111), as obtained by calculations and in experiment.

In our MD simulations, the diffusion of the Cu monomer on Ag(111) also involves recrossings[48] as well as long ($\sim$2.89 Å) $f \rightarrow f$ hops and yet longer hops[20] even at 300 K. Long jumps, in fact, occur as often as short ($\sim$1.67 Å) $f \rightarrow h$ hops at 500 and 700 K even though they necessarily occur via consecutive $f \rightarrow h$ hops (with a residence time of less than 0.1 ps).

Our calculated effective energy barrier from MD simulations (in Table I) is in reasonable agreement with the experimental value, 65 ± 9 meV.[35] Notice, however, that the slight difference between the two values could be related to the fact that the experimental barrier pertains mainly to $f \leftrightarrow f$ hoping whereas that from MD simulations stems largely from $f \leftrightarrow h$ hoping. Therefore, if the barrier for $f \leftrightarrow h$ hopping is lower than that for $f \leftrightarrow f$ hopping,[11,36,37] it is plausible to expect that $f \leftrightarrow h$ hops slightly bias our computed effective energy barrier toward lower values.

Both experiment[22,35,49–51] and theory[11,36,37,39] concur that the effective barrier for monomer diffusion is lower on Cu(111) than on Ag(111) (see Fig. 4). Such a result was unexpected since it is fair to assume that the binding energy of a Cu monomer on Ag(111) is slightly smaller than that on Cu(111).[53] Along these lines, one would hence expect the monomer diffusion barrier to be slightly smaller on Ag(111) than on Cu(111), as in the case of the dimer (Fig. 4) and larger islands.[59] As we shall see, this particular case, nonetheless, seems rather to be determined by the mismatch between the typical bond lengths of the Cu adatom and the Ag substrate, which, essentially, constrains the diffusion of Cu monomers to steps $\sim$10% longer than those prescribed on Cu(111). Kürpick and Rahman[28,57] have in fact noted for Cu, Ni, and Ag(001) surfaces that the energy barriers for adatom self-diffusion via hopping increase ($\sim$10 meV) as the lattice expands (by less than 2%).

B. Dimer

The diffusion processes of dimers on (111) surfaces can be classified into intracell and intercell processes.[22,37,49] Any dimer can be considered to lie inside a hexagonal cell which

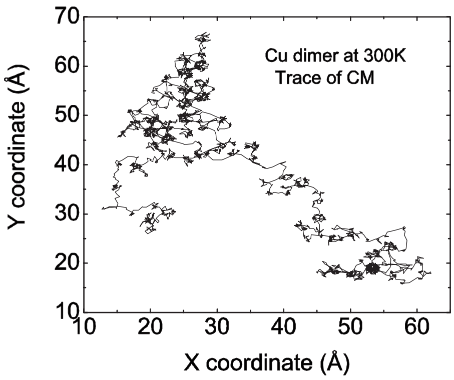

FIG. 5. Trace of the center of mass of the Cu dimer on Ag (111) at 300 K for 2000 ps.

is delineated by the six-surface NN atoms of a seventh surface atom. Intracell processes are those which occur inside a single cell, whereas intercell processes shift the dimer to another cell.

The movies generated from our MD simulations[54] show that such intracell processes (these can be zigzag motion, concerted rotations, and short concerted translations) predominate in the kinetics of the Cu dimer on Ag(111) (see Fig. 5). The rate of intercell mechanisms is, however, not much lower than that of intracell mechanisms. These often occur via intercell zigzag or concerted jumps. Translational concerted hops with rotation are considerably less frequent. Sudden multiple translational or rotational concerted jumps resembling a barrierless sliding motion—"long jumps"—are rarer yet but nevertheless occasionally present at 700 K. (Still, as shown in Fig. 5, the dimer performs long jumps even at 300 K in the sense of consecutive intercell mechanisms with residence times shorter than 0.1 ps.)

Before turning to a detailed analysis of the observed processes, we find it useful, for highlighting the dissimilarities between the homoepitaxial and heteroepitaxial systems, to compare their diffusion energetics. Our calculated effective diffusion barrier for the Cu dimer on Ag(111) is 73 meV, in excellent agreement with experiment.[35] This value is hence ~0.5 times that calculated[35] for the concerted motion by molecular statics and, more importantly, 0.6 times that for the ff-fh zigzag motion proposed by Morgenstern *et al.* in Ref. 35. In the homoepitaxial case, on the other hand, the calculated effective diffusion barrier of a Cu dimer on Cu(111) is very close to that of a dimer for the (ff-hh) concerted motion (100–130 meV) (Refs. 11, 36, and 37) and much larger than that for intracell ff-fh zigzag mechanisms (~30 meV or less).[36,37,49] Thus, keeping in mind that various calculations indicate that the concerted motion dominates the diffusion of Cu dimers on Cu(111),[11,36,37] the contrast exposed above suggests the presence and importance of diffusion mechanisms in the heteroepitaxial case which are different from the ff-fh zigzag proposed in Ref. 35 and from the concerted motion of a Cu dimer on Cu(111).[36] On the experimental side,[22,35] Cu dimers on Ag(111) were observed to move intracellularly at 16 K. The onset of the Cu dimer formation was nevertheless detected only above 19 K. Intercell diffusion on Ag(111) was detected experimentally only above 24 K. For the homoepitaxial case, Repp *et al.* determined that the onset of dimer formation on Cu(111) takes place above 19 K—just as it does on Ag(111). Dimers on Cu(111) start to diffuse above 21 K,[49,51]—i.e., at a temperature 3 K lower than that at which the intercell diffusion on Ag(111) was observed.[22,35] Their diffusion barrier, nevertheless, has not been determined since monomers and dimers disappear at 22 K.[51,52] It is remarkable, though, that in spite of the fact that intracell rotation of Cu dimers (*preassembled* via atomic manipulation) on Cu(111) is triggered at ~5 K,[49] such a *premature* onset does not assist the intercell diffusion at all. We shall come back to this point of comparison between the homoepitaxial and heteroepitaxial cases in Sec. IV B.

As we have seen above, the MD effective diffusion barrier for the Cu dimer is significantly lower on Ag(111) (by ~40 meV) than on Cu(111) and thus inverts the trend found for the monomer. This peculiarity therefore unfolds another fundamental feature of heteroepitaxy (apart from the lattice mismatch) which comes into play as soon as a Cu-Cu bond is present. Namely, the slight bond-strength disparity between homobonds and heterobonds influences the diffusivity of the Cu dimer on Ag(111) and leads to a dimer kinetics significantly different from that in the homoepitaxial case. Cu atoms, for instance, may optimize the Cu-Ag bond lengths by sitting on ideal f (or h) sites—the lowest energy sites for the monomer—[22] while separated from each other by a length almost as large as the bulk Ag bond length (2.89 Å). On the other hand, they may rearrange themselves so as to shorten their bond length to, say, something close to that of bulk Cu (2.55 Å), at the expense of breaking Cu-Ag bonds. As expected,[53] the second scenario preponderates in our simulations. However, the finite temperature of the system in our MD simulations causes both scenarios to alternate, giving rise to an in-plane vibration of the Cu-Cu bond that effectively assists the kinetics of the dimer (both rotation and translation) and subjects the substrate to an alternate "contraction-relaxation" motion.

In the rest of this section we detail the configurations and processes observed for the Cu dimer on Ag(111) in our MD simulations. Ideal ff (or hh) lattice sites are rarely observed in our simulations. Such sites are stabilized within a locally buckled Ag(111) surface that preserves a small Cu-Cu bond, albeit with a lifetime shorter than that of monomers at f sites. More complex off-lattice configurations, for their part, appear frequently, perhaps closely competing as low-energy adsorption sites. Although such sites involve dislocations on the Ag(111) surface, they can be described as hb-, fb-, bb- and short-axis fh-like sites. We observe that these dimer configurations substantially stretch one of the Cu-Ag bonds. The dimer is thus often effectively bound to only four surface atoms rather than five.

Our MD simulations show that dimer rotations are actually more frequent than monomer hopping. The appearance of off-lattice sites for dimers thus counteracts the lattice mismatch effect that hinders the diffusion of the monomer. The reason is that dimer processes are not necessarily constrained by the relatively *long* (2.89 Å) Ag-bond-length jumps. Zigzag processes are not limited to ff-fh (long-axis)-hh sequences provided, apparently, that hb- and fb-like sites are

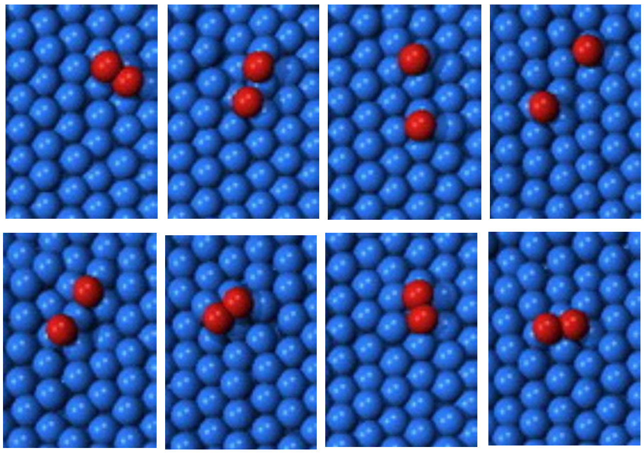

FIG. 6. (Color online) Snapshots of the dimer diffusion in our MD simulation at 700 K. The figure illustrates that the Cu dimer occasionally dissociates at 700 K, though the constituting atoms recombine after a few picoseconds.

local minima too. One important consequence of the latter feature is that the zigzag processes on Ag(111) not only displace the dimer inside a cell but also execute intercell translations. That is, the dimer's diffusion is often a consequence of numerous intracell (zigzag or rotational) processes, which may displace the dimer within a cell through hb-, fb-, ff-, hh-, bb- and fh-like sites, and set the dimer up for departing the cell via a concerted jump or a zigzag step (see Fig. 5). In summary, off-lattice configurations empower the above-mentioned diffusion mechanism, which in turn seem to account for the low effective diffusion barrier of the Cu dimer on Ag(111), relative to both that of the monomer on Ag(111) and of the Cu dimer on Cu(111).

The dissociation of the dimer is observed a few times at 700 K (see Fig. 6 and Ref. 54). This process occurs after the occupation of hh and long-axis fh sites. Reattachment occurs a few picoseconds later. It is worth noting that Cu dimer dissociation has not been reported so far on Cu(111) in MD or kinetic Monte Carlo simulations.[36–39] The static barrier for Cu dimer dissociation on Cu(111) has been estimated to be ~410 meV.[37] From the above analysis, we infer that the barrier for the Cu dimer dissociation is reduced on Ag(111) because of the lattice mismatch and the close competition between the almost equally strong Cu-Cu and Cu-Ag bonds.[53]

As the dimer vibrates, rotates, and diffuses during the incessant struggle between optimizing Cu-Cu or Cu-Ag bonds, the *soft* Ag substrate responds elastically to the varying off-lattice configurations of the dimer and undergoes larger dislocations than those observed during the diffusion of the monomer (see above). Some of the most common dislocations induced by the Cu dimer—apart from the expansion of the nearest Ag-Ag bonds of those Ag atoms that make bonds with Cu atoms—are the downward shift of a given Ag atom and the upward shift of its Ag NN when the center of mass of the Cu dimer passes above the former. Finally, as the Cu dimer diffuses at 700 K, its Ag neighbors may vibrate as though trying to follow one of the Cu atoms by popping out of the surface [a feature observed indeed in simulations[59] for a Cu trimer on Ag(111)].

IV. *AB INITIO* DIFFUSION ENERGETICS: RESULTS AND DISCUSSION

In this section we present the diffusion energetics of the Cu monomer and dimer on Ag(111) from our first-principles calculations. As in the previous section, our analysis resorts to comparison with the homoepitaxal case, which has been studied earlier by Repp *et al.*[49] Still, for the sake of consistency in comparing two *ab initio* calculations and because we need relevant bond lengths not provided in their work, we have repeated some key calculations of the Cu monomer and dimer energetics on Cu(111).

A. Monomer

Our first-principles calculations confirm that Cu monomers are more stable at fcc (2.498 eV) sites than at hcp (2.492 eV). There is a small adsorption energy difference between fcc and hcp sites of 6 meV, in excellent agreement with that revealed by experiment of 5.5 ± 1.0 meV.[35] The bridge site is not a local minimum of the potential-energy surface. In fact, the bridge configuration is very close to the transition state (2.423 eV) between fcc and hcp sites.

Our calculated barrier for Cu monomers to diffuse from an hcp site to an fcc site is 69 meV and that of the inverse process is 75 meV, both of which are in very good agreement with the experimental effective activation barrier (65 ± 9 meV) (Ref. 35) and ~13 meV higher than those of our MD calculations (see Table I). Our result together with that of Ref. 49 tells us that DFT calculations also predict that the diffusion barrier of a Cu monomer on Cu(111) (50 meV from fcc to hcp) is smaller than that on Ag(111) (see Sec. III A) by ~25 meV. As assumed in Sec. III A, although pure considerations of bond-strength point to the opposite behavior, an analysis of the bond lengths involved explains straightforwardly why the diffusion barrier for Cu monomers is higher on Ag(111) than on Cu(111): the Cu monomer at an fcc site forms bonds with its three Ag NN slightly shorter (2.57 Å) than the DFT bulk Cu bond length (2.58 Å) since it is not constrained by other Cu-Cu bonds in any direction.[53] Likewise, at the fcc-hcp transition state (see Fig. 7) the "unconstrained" Cu monomer makes quite "short" bonds of 2.51 Å with two Ag atoms plus two rather "long" bonds, of 3.01 Å, with other two Ag atoms. Here, it is important to notice that the latter bonds are dictated by the typical bond length of the substrate ~2.90–3.01 Å, as shown in Fig. 7. Similar circumstances hold for Cu/Cu(111). Yet, while on Ag(111) the long Cu-Ag bonds at the transition state significantly quench the Cu-Ag interaction and thus barely contribute to the binding energy of the Cu monomer at this site, on Cu(111) the long bonds (2.72 Å) add much more to the monomer binding energy. In order to test the above argument, it would be well to examine more closely the geometry of Cu/Ag(111) at the fcc and the transition-state sites by replacing the Ag atoms by Cu atoms (resulting in an expanded Cu substrate). Let us also imagine that the Cu monomer is free to relax and get as close as possible to its Cu neighbors at both the fcc and transition-state sites. In this case, one finds that the barrier increases to 128 meV. This is because the strength and length of the bond are correlated:

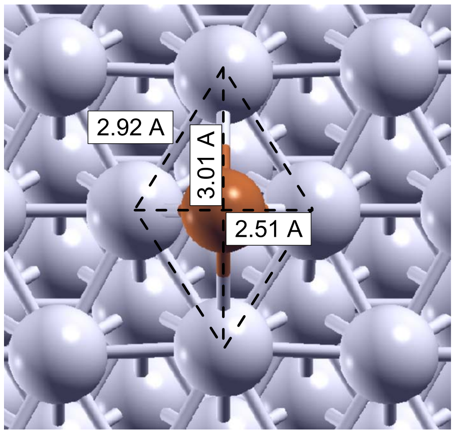

FIG. 7. (Color online) Local coordination of a Cu monomer (dark gray ball or orange ball in online version) at the transition state of the diffusion from fcc to hcp on Ag(111) (light gray balls) according to our DFT calculations. Labels show the distances between the Cu adatom and its four NN (2.51 and 3.01 Å). The distance among its Ag NN is also displayed (2.92 Å).

specifically the *d* orbitals of Cu are shorter than those of Ag and, even though the Cu-Cu interaction is stronger than the Ag-Ag and Cu-Ag interactions, it dies off faster with increasing distances.[53] The difference in energy barrier for a Cu monomer between Ag(111) and Cu(111) is thus related to the characteristic bond length of the underlying substrate, regardless of the fact that the binding energy of a Cu monomer on Ag(111) is lower than on Cu(111).

B. Dimer

Our DFT calculations indicate that Cu dimers adsorb more favorably at ff sites than at hh sites by an energy difference of 13 meV (see Fig. 8). As suggested by our MD simulations, a key feature of the Cu dimer on Ag(111) is the preference of Cu atoms to rearrange themselves so as to shorten their bond lengths close to, say, that of bulk Cu, even at the expense of enlarging some Cu-Ag bonds. We find indeed that for each atom in the dimer at ff and hh sites, one of the NN Ag atoms is at a distance of 2.56 Å, shorter than the bond length of bulk Cu; one is at a distance almost equal to bond-length of bulk Cu, 2.59 Å; and another is stretched to a distance of 2.68 Å. The dimer in ff and hh configurations thus does not reside strictly at ff or hh sites. Also, we note that the Cu-Cu bond at ff and hh sites is significantly shortened with respect to the bond length in bulk Cu (from ~2.58 Å in bulk to 2.48 Å and 2.46 Å, respectively). The mismatch with the Ag substrate therefore becomes even more pronounced. The above two features thus account for the apparent off-lattice sites observed for the dimer in our MD simulations since the Cu atoms forming the dimer are located close to bridge sites (see Fig. 8). The Cu dimer at fb and hb sites is actually not stable but relaxes, respectively, to an ff and to an hh site. Note that these results are for zero-temperature and, unlike our MD simulations, provide information of the lowest energy configuration only: that which optimizes the Cu-Cu bond. Our DFT calculations thus cannot tell us about the competing configuration in which each atom optimizes three Cu-Ag bonds; neither can they tell us about any processes that may take place because of the competition between optimizing one Cu-Cu bond plus four Cu-Ag bonds and optimizing six Cu-Ag bonds (see Sec. III B). The bb site (when both atoms site at bridges sites along one of the [110]-type directions) is not a local minimum but rather the transition state for a concerted motion of the dimer from ff to hh (see Fig. 9). The energy barrier for the concerted motion from ff to hh is 159 meV and that for the reverse process is 146 meV. Since these barriers are twice those for the monomer, our rationale for their value follows what we outlined above for the energy barrier of the monomer. The fact that the barrier for this ff-to-hh concerted motion is significantly higher than the effective barrier predicted on experimental grounds and by our MD simulations suggests that other mechanisms dominate the diffusion of the dimer on Ag(111).

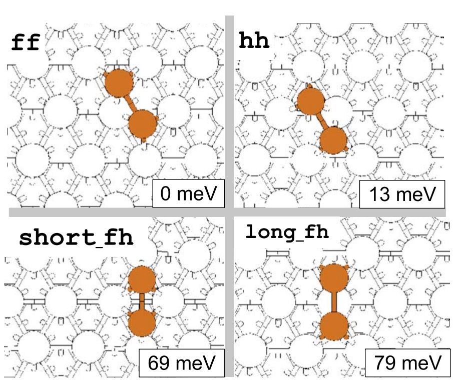

FIG. 8. (Color online) Local minima of the potential-energy surface of a Cu dimer on Ag(111) found by our DFT calculations (see text). The abbreviations f and h correspond to the hollow sites where Cu atoms sit and stand for fcc and hcp, respectively. The energy at the bottom-right corner of each configuration is the total energy of the corresponding configuration. Note that the zero of the total energy has been arbitrarily set at the energy of the dimer at the ff configuration, which has lowest energy.

Our DFT calculations show four diffusion mechanisms for the Cu dimer on Ag(111) different from the zigzag (from ff to long_fh [see Fig. 8]) and concerted motions reported in Refs. 11, 36, 37, and 49 for the Cu dimer on Cu(111), as expected from our MD simulations. These are from ff to short_fh (see Fig. 8) and the inverse mechanism plus that from hh to short_fh and its inverse mechanism (see Fig. 9). Before we continue, a word of caution is in order. Considering both the short_fh and the long_fh configurations as local minima instead of transitions states may be questionable since we found them to be only ~4 meV below the transition state to the ff site (see Fig. 9), a value which is close to the error bar of our calculation. As a matter of fact, the potential-energy surface for the diffusing atom around both the short_fh and the long_fh configurations is fairly flat. For example, the energy may vary only by ~10 meV when the diffusing atom moves by ~0.5 Å. Whichever may be the better designation of these two configurations, we shall see that it is beyond any doubt that the short_fh configuration enables intercell diffusion with a relatively low-energy barrier, compared with that of the ff-hh concerted motion of the Cu dimer on both Cu(111) (Ref. 36) and Ag(111) (Fig. 9).

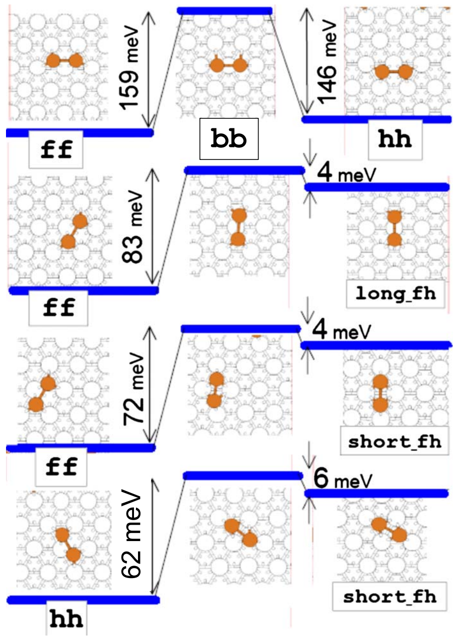

FIG. 9. (Color online) Energy barriers for four diffusion processes of a Cu dimer on Ag(111) obtained by our DFT calculations (see text). The atomic configurations of the dimer at the initial, transition, and final states are shown from left to right. The abbreviations f, h, and b correspond to the sites where Cu atoms sit and stand for fcc, hcp, and bridge, respectively. We do not give a distinct name to the various transition states since their configuration is off-lattice, except for the transition state of the first case, which is the bb configuration.

From the DFT calculations by Repp *et al.*[49] on Cu(111) and the present calculations, one can conclude that the shape of the potential-energy surface for the Cu dimer on Ag(111) is in general significantly different from that of the Cu dimer Cu(111). Two main contrasting features between diffusion on Cu(111) and on Ag(111) are the following: (1) the short_fh configuration tends to bring the two Cu atoms extremely close to each other. The substrate thus needs to be strained in order to hold the two atoms at a distance of at least 2.38 Å from each other, increasing the energy by 130 meV with respect to that obtained at the ff adsorption site. [We performed this calculation since the short_fh configuration was not even considered on Cu(111) by Repp *et al.*] On Ag(111), in turn, even though short_fh is the configuration for which the bond length of the Cu dimer is also shortest (2.38 Å), its energy is lower than that of the long_fh site (Fig. 8). (2) While the total energy of the dimer in the long_fh configuration on Cu(111) is very close to that of the ff configuration[36,37,49] (24 meV according to our calculation), the corresponding energy difference on Ag(111) is 79 meV.

Let us now turn to the energy barriers for the diffusion of the Cu dimer on Ag(111). The barriers from ff to short_fh and from ff to long_fh are 72 meV and 83 meV, respectively. These are the key barriers of ff↔short_fh and ff↔long_fh processes since the barriers for the inverse hops are only 4 meV (see Fig. 9). Likewise, the barrier from hh to short_fh is 62 meV and that of the inverse process is only 6 meV (Fig. 9). The key energy barriers for the above-mentioned pro-

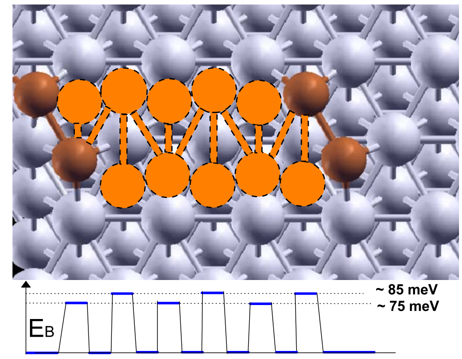

FIG. 10. (Color online) Sequence of diffusion processes exemplifying how alternation of the ff-short_fh and the ff-long_fh processes may assist intercell diffusion by zigzag steps that require energies of ~80 meV. At the bottom we show the energy-barrier profile that the dimer may encounter in such sequences of processes.

cesses, incidentally, fit nicely to the effective activation energy barrier for the diffusion of the dimer obtained by experiment and by our MD calculations (73 meV). We also note that these barriers are much lower than that of the zigzag intercell mechanism proposed by Morgenstern *et al.*[35] Furthermore, by comparing these values with the barriers for the monomer, one could account for the dominance of intracell dimer rotation over monomer diffusion in our MD simulations.

Since the long_fh configuration is energetically fairly favorable for the Cu dimer on Cu(111) with respect to the ff site (see above), it has been possible to excite the intracell rotation of the Cu dimer on Cu(111) by thermally assisted tunneling at ~5 K.[49] But since the short_fh site has an energy 130 meV higher than that of the ff site, and since the dimer cannot do much more than ff-long_fh rotations at that temperature, it is thus confined to remaining within a cell. The Cu dimer therefore does not diffuse until it can overcome the barrier for the ff-hh concerted motion.[36] The situation is different for a Cu dimer on Ag(111) since the energy of both the long_fh and the short_fh lies ~60–80 meV above that of the ff and hh sites. Consequently, the rotation is not triggered until the temperature reaches 16 K. The importance of the short_fh configuration of a Cu dimer on Ag(111), however, concerns not only the identification of one more intracell process possible in heterogeneous systems, but also the fact that, acting together with the processes involving the long_hp sites, they may give rise to intercell diffusion merely via zigzag steps of relatively low energy, along the [110]-type directions (see, e.g., Fig. 10). Hence, since the stability of the short_fh is established by the relatively large Ag-Ag bonds, one can say that the long bonds of the substrate atoms favor the dimer diffusion.

Another consequence of the existence of the short_fh configuration is that the ff-hh concerted motion that dominates the intercell diffusion of the dimer on Cu(111) [see Ref. 36 and its Fig. 4(b)] does not exist on Ag(111) as such but splits as an ff-short_fh-hh process. The reason is that, since no Ag atom lies below and between the two Cu atoms (see e.g., the bb site in Fig. 8), as soon as the Cu atoms start to depart from their fcc sites, the Cu-Cu bond shortens and the dimer gets trapped in a short_fh configuration.

To conclude, we highlight that our DFT results show that EAM potentials and MD simulations are able to capture that: (1) dimer processes are not necessarily constrained by the relatively *long* (2.89 Å) Ag-bond-length jumps; (2) optimization of the Cu-Cu and the Cu-Ag bond lengths is energetically more favorable than optimization of Ag-Ag bonds; (3) zigzag processes on Ag(111) are not limited to ff↔long_fh↔hh sequences as on the Cu(111) surface; (4) these zigzag processes not only displace the dimer inside a cell but also execute intercell translations; and (5) local minima not present on Cu(111) boost the dimer diffusion on Ag(111). It would not be surprising that processes such as that shown in Fig. 10 largely correspond to the multiple translational concerted jumps that resemble a barrierless sliding motion in our MD simulation.[54]

V. SUMMARY

We have studied the diffusion of the Cu monomer and dimer on Ag(111) surface using many-body interatomic potentials developed by Foiles *et al.*[42] Our MD calculations indicate the effective energy barriers to be 59 and 73 meV for the monomer and dimer, respectively, the latter in excellent agreement with experiment. Our DFT calculations determine that the fcc-to-hcp and the hcp-to-fcc energy barriers for the monomer are 75 meV and 69 meV, respectively, in agreement with our MD calculations and with experiment. For the dimer, our DFT calculations find that the presence of the short fcc-hcp configuration with its relatively low-energy triggers processes that may act together with those involving the long fcc-hcp site to establish an *efficient* intercell zigzag diffusion. The former processes involve energy barriers of ~72 meV at most and are not favorable for the Cu dimer on Cu(111). In turn, the latter processes involve energy barriers of 83 meV and do exist for the Cu dimer on Cu(111) at even much lower energies.

From our DFT calculations we conclude that the relatively high barrier for a Cu monomer on Ag(111) with respect to that on Cu(111) is due to the lattice mismatch, since Cu monomers on Ag(111) diffuse through hops ~10% longer than those they exhibit on Cu(111), which make them detach significantly from other Ag NN at the transition state. In the case of the dimer, nevertheless, the relatively long bond length of the substrate now works to empower diffusion routes (fcc-to-short_fh-to-fcc) not energetically favorable in the homoepitaxial case, Cu/Cu(111). By in this way screening the lattice-mismatch effect that hinders monomer diffusion, such processes account for the low effective diffusion barrier of the Cu dimer on Ag(111), relative to that of Cu dimers on Cu(111).

Our MD simulations also suggest that at finite temperatures the close similarity between Cu-Cu and Cu-Ag bonds in respect to bond strength and bond length promotes off-lattice sites and establishes a competition between the optimization of these two types of bonds, resulting in an in-plane Cu-Cu vibration that assists the kinetics of the dimer (including dissociation at 700 K) and subjects the substrate to an alternate *strain-release* motion. Along these lines, it is tempting to speculate that the Ag-Cu lattice mismatch and the bond-optimization hierarchy[53] (among homobonds and heterobonds) that minimizes the energy may establish the dimer as the turning point of a generalized enhanced mobility of Cu islets on Ag(111), as compared with that on Cu(111). Finally, we find that adatom impurities seem to be localized perturbations of the periodic potential that oscillate randomly and may generate a dynamic elastic displacement field, which falls off at long distances (~43 Å) and may be involved in the long-range monomer-dimer and dimer-dimer interactions detected in experiment.

ACKNOWLEDGMENTS

We are indebted to Altaf Karim and Lyman Baker for insightful discussions and numerous helpful suggestions during the preparation of this manuscript. The work of S.S.H. was supported by the IRSIP of the Higher Education Commission (HEC) of Pakistan. M.A.O. and T.S.R. were supported in part by U.S.-NSF under Grant No. 0840389. Calculations were carried out at the Department of Physics, University of Central Florida.

*Present address: Department of Physics and Astronomy, Hazara University Mansehran (NWFP), Pakistan; sikandariub@yahoo.com
†drmarshadch@yahoo.com
‡alcantar@physics.ucf.edu; mortigoz@mail.ucf.edu
§talat@physics.ucf.edu

[1] K. Kern, R. David, R. L. Palmer, G. Comsa, J. He, and T. S. Rahman, Phys. Rev. Lett. **56**, 2064 (1986).
[2] K. Kern, H. Niehus, A. Schatz, P. Zeppenfeld, J. Goerge, and G. Comsa, Phys. Rev. Lett. **67**, 855 (1991).
[3] J. Bork, P. Wahl, L. Diekhöner, and K. Kern, New J. Phys. **11**, 113051 (2009).
[4] S. Stolbov, M. Alcántara Ortigoza, and T. Rahman, J. Phys.: Condens. Matter **21**, 474226 (2009).
[5] K. Kyuno and G. Ehrlich, Phys. Rev. Lett. **84**, 2658 (2000).
[6] S. C. Wang and G. Ehrlich, Phys. Rev. B **65**, 121407(R) (2002).
[7] T. R. Linderoth, S. Horch, L. Petersen, S. Helveg, M. Schonning, E. Laegsgaard, I. Stensgaard, and F. Besenbacher, Phys. Rev. B **61**, R2448 (2000).
[8] A. M. Cadilhe, C. R. Stoldt, C. J. Jenks, P. A. Thiel, and J. W. Evans, Phys. Rev. B **61**, 4910 (2000).
[9] T. R. Linderoth, S. Horch, L. Petersen, S. Helveg, E. Laegsgaard, I. Stensgaard, and F. Besenbacher, Phys. Rev. Lett. **82**, 1494 (1999).
[10] F. Montalenti and R. Ferrando, Phys. Rev. Lett. **82**, 1498 (1999).
[11] C. M. Chang, C. M. Wei, and S. P. Chen, Phys. Rev. Lett. **85**, 1044 (2000).
[12] X. F. Gong, B. Hu, X. J. Ning, and J. Zhuang, Thin Solid Films

493, 146 (2005).
[13] A. N. Al-Rawi, Ph.D. thesis, Kansas State University, 2005.
[14] F. Montalenti and R. Ferrando, Phys. Rev. B **59**, 5881 (1999).
[15] H. Bulou and C. Massobrio, Phys. Rev. B **72**, 205427 (2005).
[16] Y. Shim and J. G. Amar, Phys. Rev. B **73**, 035423 (2006).
[17] B. H. Aguilar, J. C. Flores, A. M. Coronado, and H. Huang, Modell. Simul. Mater. Sci. Eng. **15**, 419 (2007).
[18] C. Polop, A. Lammerschop, C. Busse, and T. Michely, Phys. Rev. B **71**, 125423 (2005).
[19] D. Chen, W. Hu, J. Yang, and L. Sun, J. Phys.: Condens. Matter **19**, 446009 (2007).
[20] G. Antczak and G. Ehrlich, Surf. Sci. Rep. **62**, 39 (2007).
[21] H. Brune, Surf. Sci. Rep. **31**, 125 (1998).
[22] K. Morgenstern and K. L. Rieder, New J. Phys. **7**, 139 (2005).
[23] F. Bocquet, C. Maurel, J. M. Roussel, M. Abel, M. Koudia, and L. Porte, Phys. Rev. B **71**, 075405 (2005).
[24] C. Goyhenex, Surf. Sci. **600**, 15 (2006).
[25] S. D. Borisova, S. V. Eremeev, G. G. Rusina, V. S. Stepanyuk, P. Bruno, and E. V. Chulkov, Phys. Rev. B **78**, 075428 (2008).
[26] L. Vitos, A. V. Ruban, H. L. Skriver, and J. Kollár, Surf. Sci. **411**, 186 (1998).
[27] A. Kara, O. Trushin, H. Yildirim, and T. S. Rahman, J. Phys.: Condens. Matter **21**, 084213 (2009).
[28] U. Kürpick and T. S. Rahman, Phys. Rev. B **57**, 2482 (1998).
[29] L. T. Kong and L. J. Lewis, Phys. Rev. B **74**, 073412 (2006).
[30] U. Kürpick, A. Kara, and T. S. Rahman, Phys. Rev. Lett. **78**, 1086 (1997).
[31] G. H. Vineyard, J. Phys. Chem. Solids **3**, 121 (1957).
[32] M. S. Daw and M. I. Baskes, Phys. Rev. B **29**, 6443 (1984).
[33] G. Boisvert and L. J. Lewis, Phys. Rev. B **56**, 7643 (1997).
[34] B. D. Yu and M. Scheffler, Phys. Rev. B **55**, 13916 (1997).
[35] K. Morgenstern, K. F. Braun, and K. H. Rieder, Phys. Rev. Lett. **93**, 056102 (2004).
[36] A. Karim, A. N. Al-Rawi, A. Kara, T. S. Rahman, O. Trushin, and T. Ala-Nissila, Phys. Rev. B **73**, 165411 (2006).
[37] M. C. Marinica, C. Barreteau, M. C. Desjonquères, and D. Spanjaard, Phys. Rev. B **70**, 075415 (2004).
[38] J. Yang, W. Hu, J. Tang, and M. Xu, J. Phys. Chem. C **112**, 2074 (2008).
[39] J. Tang, M. Xu, X. Li, and W. Long, Chin. J. Chem. Phys. **21**, 27 (2008).
[40] W. H. Press, S. A. Teukolsky, W. T. Vetterling, and B. P. Flannery, *Numerical Recipes in Fortran: The Art of Scientific Computing*, 2nd ed. (Cambridge University Press, Cambridge, 1992).
[41] A. Nordsieck, Math. Comput. **16**, 22 (1962).
[42] S. M. Foiles, M. I. Baskes, and M. S. Daw, Phys. Rev. B **33**, 7983 (1986).
[43] M. Payne, M. Teter, D. Allan, T. Arias, and J. Joannopoulos, Rev. Mod. Phys. **64**, 1045 (1992).
[44] G. Kresse and J. Furthmuller, Phys. Rev. B **54**, 11169 (1996).
[45] H. Monkhorst and J. Pack, Phys. Rev. B **13**, 5188 (1976).
[46] J. P. Perdew, K. Burke, and M. Ernzerhof, Phys. Rev. Lett. **77**, 3865 (1996).
[47] L. Yang and T. S. Rahman, Phys. Rev. Lett. **67**, 2327 (1991).
[48] J. Ferrón, L. Gómez, J. J. de Miguel, and R. Miranda, Phys. Rev. Lett. **93**, 166107 (2004).
[49] J. Repp, G. Meyer, K. H. Rieder, and P. Hyldgaard, Phys. Rev. Lett. **91**, 206102 (2003).
[50] J. Repp, F. Moresco, G. Meyer, K. H. Rieder, P. Hyldgaard, and M. Persson, Phys. Rev. Lett. **85**, 2981 (2000).
[51] N. Knorr, H. Brune, M. Epple, A. Hirstein, M. A. Schneider, and K. Kern, Phys. Rev. B **65**, 115420 (2002).
[52] J. A. Venables and H. Brune, Phys. Rev. B **66**, 195404 (2002).
[53] M. Alcántara Ortigoza and T. S. Rahman, Phys. Rev. B **77**, 195404 (2008).
[54] http://sites.google.com/site/mdresearchproject/
[55] http://www.kettering.edu/drussell/Demos/radiation/radiation.html
[56] P. J. Feibelman, Phys. Rev. B **55**, 8821 (1997).
[57] U. Kürpick and T. S. Rahman, Surf. Sci. **427-428**, 15 (1999).
[58] A. Khater, N. Auby, and D. Kechrakos, J. Phys.: Condens. Matter **4**, 3743 (1992).
[59] S. S. Hayat, M. A. Choudhry, M. A. Alcántara Ortigoza, and T. S. Rahman (unpublished).